open-circuit coupled line. Therefore, the admittance inverters J_{12} and J_{23} of the transmission lines Z_2, and the even- and odd-mode coupled line admittances Y_{0e} and Y_{0o} can be expressed as

$$J_{12} = J_{34} = Y_2 \csc \theta_2 \quad (1)$$

$$\frac{Y_{0e}}{Y_3} = 1 - \frac{J_{23}}{Y_3}\cot \theta_3 \quad (2)$$

$$\frac{Y_{0o}}{Y_3} = 1 + \frac{J_{23}}{Y_3}\cot \theta_3 \quad (3)$$

where Y_i's are the inverse of Z_i's and Y_3 is the corresponding admittance of the symmetrical open-circuit coupled line.

For the simplified filter, center frequency, ripple and fractional bandwidth are set as 2 GHz, 0.01 dB, and 5%, respectively. Here, the electrical lengths θ_1, θ_3 and impedance Z_3 are set as an example with 68.7°, 19.1°, and 10.1 Ω, respectively. Then, the impedances Z_1, Z_2, Z_{0e}, and Z_{0o} and electrical length θ_2 of the simplified bandpass filter are obtained as 17.78 Ω, 76.4 Ω, 10.51 Ω, 9.72 Ω, and 26°, respectively.

These theoretical values are converted to dimensions of the wide-stopband bandpass filter, which is designed on the substrate Rogers RO4003 whose dielectric constant, loss tangent, and thickness are 3.38, 0.0027, and 0.508 mm, respectively. Figure 3 shows the comparison of results between EM simulation and theoretical prediction for the wide-stopband microstrip bandpass filter. In the EM simulation, the larger harmonic appears at the frequency band of 20 GHz, which may extend the stopband to $10f_0$ while the insertion loss is greater than 28 dB. To achieve a very wide stopband, patterned ground plane is utilized to design a bandpass filter.

By using patterned ground plane, a wider stopband will appear. In Figure 4, the patterned ground plane causes the stopband to extend to 50 GHz while the insertion loss greater than 18 dB. Moreover, the increased transmission-line impedance by patterned ground plane can also shift the center frequency of the passband downward.

3. EXPERIMENTAL RESULTS

A new microstrip bandpass filter has been developed to generate a very wide stopband. The center frequency, fractional bandwidth, and ripple of this bandpass filter are set at 1 GHz, 18%, and 0.01 dB, respectively. The dimensions of this filter, as shown in Figure 1, are: $L_1 = 11.9$ mm, $L_2 = 4.45$ mm, $L_3 = 3$ mm, $L_4 = 1.4$ mm, $L_5 = 4.45$ mm, $L_6 = 0.8$ mm, $L_7 = 8.4$ mm, and $L_S = 3.3$ mm, $W_1 = 2$ mm, $W_2 = 0.2$ mm, $W_3 = 0.4$ mm, $W_S = 0.3$ mm, $G = 0.2$ mm, $S_1 = 6.2$ mm, $S_2 = 5.4$ mm, $S_3 = 12.3$ mm, and $S_4 = 5.2$ mm. Moreover, the photograph of the new filter and a comparison of the measured and EM simulation responses are shown in Figure 5.

Figure 5(b) points out that the measured stopband of the bandpass filter extends to 50 GHz with the insertion loss greater than 23.5 dB, and the harmonic frequency of the proposed bandpass filter shifts to over 50 times of the fundamental frequency f_0. This feature is applicable to both the EM simulation and measurement. In addition, Figure 5(b) indicates that within the passband of 0.9–1.1 GHz the measured insertion loss is less than 0.6 dB while the measured return loss is greater than 17 dB.

4. CONCLUSION

A new approach to generate a very wide stopband, from 1.53 to 50 GHz, in the microstrip bandpass filter is proposed. The measured harmonic suppression of the bandpass filter is more than 23.5 dB. The fabricated filter demonstrates the potential for harmonic suppression with the assistance of patterned ground plane. Moreover, excellent agreement between theoretical and measured results validates the proposed structure.

ACKNOWLEDGMENTS

This work was supported in part by the National Science Council of Taiwan, Republic of China, under grant NSC 98-2221-E-194-016.

REFERENCES

1. S.B. Cohn, Parallel-coupled transmission-line-resonator filters, IRE Trans Microwave Theory Tech MTT-6 (1958), 223–231.
2. J.T. Kuo, S.P. Chen, and M. Jiang, Parallel-coupled microstrip filters with over-coupled end stages for suppression of spurious responses, IEEE Microwave Wireless Compon Lett13 (2003), 440–442.
3. T. Lopetegi, M.A.G. Laso, J. Hernández, M. Bacaicoa, D. Benito, M.J. Garde, M. Sorolla, and M. Guglielmi, New microstrip wiggly-line filters with spurious passband suppression, IEEE Trans Microwave Theory Tech49 (2001), 1593–1598.
4. M. Makimoto and S. Yamashita, Bandpass filters using parallel coupled stripline stepped impedance resonators, IEEE Trans Microwave Theory Tech28 (1980), 1413–1417.
5. C.W. Tang and H.H. Liang, Parallel-coupled stacked SIRs bandpass filters with open-loop resonators for suppression of spurious responses, IEEE Microwave Wireless Compon Lett15 (2005), 802–804.
6. S.Y. Lee and C.M. Tsai, New cross-coupled filter design using improved hairpin resonators, IEEE Trans Microwave Theory Tech48 (2000), 2482–2490.
7. J.G. Garía, F. Martín, F. Falcone, J. Bonache, I. Gil, T. Lopetegi, M.A.G. Laso, M. Sorolla, and R. Marqués, Spurious passband suppression in microstrip coupled line band pass filters by means of split ring resonators, IEEE Microwave Wireless Compon Lett14 (2004), 416–418.
8. W.H. Tu and K. Chang, Compact microstrip bandstop filter using open stub and spurline, IEEE Microwave Wireless Compon Lett15 (2005), 268–270.
9. C.W. Tang and Y.K. Hsu, A microstrip bandpass filter with ultra-wide stopband, IEEE Trans Microwave Theory Tech56 (2008), 1468–1472.

ON-BOARD 7-BAND WWAN/LTE ANTENNA WITH SMALL SIZE AND COMPACT INTEGRATION WITH NEARBY GROUND PLANE IN THE MOBILE PHONE

Kin-Lu Wong,[1] Ming-Fang Tu,[1] Chun-Yih Wu,[2] and Wei-Yu Li[2]

[1] Department of Electrical Engineering National Sun Yat-sen University, Kaohsiung 80424, Taiwan; Corresponding author: wongkl@ema.ee.nsysu.edu.tw

[2] Information and Communications Research Laboratories Industrial Technology Research Institute, Hsinchu 31040, Taiwan

Received 17 February 2010

ABSTRACT: *A small-size on-board 7-band WWAN/LTE antenna formed by a coupled-fed loop antenna connected with a chip-inductor-loaded strip is presented. The antenna is disposed on a small board space of 15 × 25 mm^2 (375 mm^2) on the system circuit board and provides two wide operating bands to respectively cover GSM850/900 (824–960 MHz) and GSM1800/1900/UMTS/LTE2300/2500 (1710–2690 MHz) for the 7-band operation in the mobile phone. The antenna's upper band is contributed by the coupled-fed loop antenna operated at its 0.5-wavelength resonant mode. The generation of the lower band is owing to the chip-inductor-loaded strip connected to the coupled-fed*

loop antenna to form a coupled-fed shorted monopole antenna operated at its 0.25-wavelength resonant mode. In addition, the antenna's lower and upper bands can be respectively controlled, making it easy in fine-tuning the desired operating bandwidths in practical applications. Further, the proposed antenna can be in compact integration with its nearby ground plane on the system circuit board; that is, small isolation distance between the antenna and the nearby ground plane can be achieved for the proposed antenna. This leads to efficient board space planning on the system circuit board of the mobile phone. Details of the proposed antenna are described in the article. © 2010 Wiley Periodicals, Inc. Microwave Opt Technol Lett 52:2847–2853, 2010; View this article online at wileyonlinelibrary.com. DOI 10.1002/mop.25619

Key words: *mobile antennas; handset antennas; small antennas; WWAN antennas; compact integration with nearby ground plane*

1. INTRODUCTION

Internal antennas that can be directly disposed on the system circuit board of the mobile phone by printing or etching are attractive for its ease in fabrication at low cost for practical applications. Some promising internal on-board antennas for the penta-band WWAN (wireless wide area network) operation in the 824–960 and 1710–2170 MHz bands have also been available [1–12]. To achieve wideband operation with a small size, these on-board WWAN antennas are required to be disposed on the no-ground board space of the system circuit board. Further, it is noted that, to accommodate the required size of these WWAN antennas (about 600 mm^2 or less), they usually occupy the whole top or bottom edges of the system circuit board, especially at the bottom edge of the circuit board such that decreased SAR values can also be achieved to meet the 1.6 W/kg SAR limit for practical mobile phone applications [10–14].

In this article, we present a novel small-size on-board mobile phone antenna to have wide operating bands to cover the 7-band operation including the WWAN operation in the GSM850/900/1800/1900/UMTS bands (824–894/880–960/1710–1880/1850–1990/1920–2170 MHz) and the LTE (long term evolution) operation [15, 16] in the LTE2300/2500 bands (2300–2400/2500–2690 MHz). The antenna is disposed on a small no-ground portion of 15 × 25 mm^2 (375 mm^2) and occupies only a fractional portion at either the top edge or bottom edge of the system circuit board. Further, the antenna can be in compact integration with the nearby ground plane at the same edge of the system circuit board. In this study, only a small isolation distance of 1 mm is needed between the antenna and the nearby ground plane on which associated electronic components in the mobile phone can be accommodated. This not only results in compact integration of the internal on-board antenna on the system circuit board, but also leads to more efficient board space planning on the system circuit board of the mobile phone.

The proposed antenna is formed by a coupled-fed loop antenna connected with a chip-inductor-loaded strip. The antenna's lower band is formed by the excited 0.5-wavelength resonant mode contributed by the coupled-fed loop antenna. While the generation of the antenna's upper band is resulted from the chip-inductor-loaded strip connected to the coupled-fed loop antenna to form a coupled-fed shorted monopole antenna operated at its 0.25-wavelength resonant mode. Owing to the chip inductor loading, which compensates for the increased capacitance with the decreasing resonant length of the monopole antenna [6, 9, 17, 18], the required length of the connected strip to generate a resonant mode at the desired 900-MHz band can be reduced; this also leads to the small size of the proposed antenna for the 7-band WWAN/LTE operation in this study.

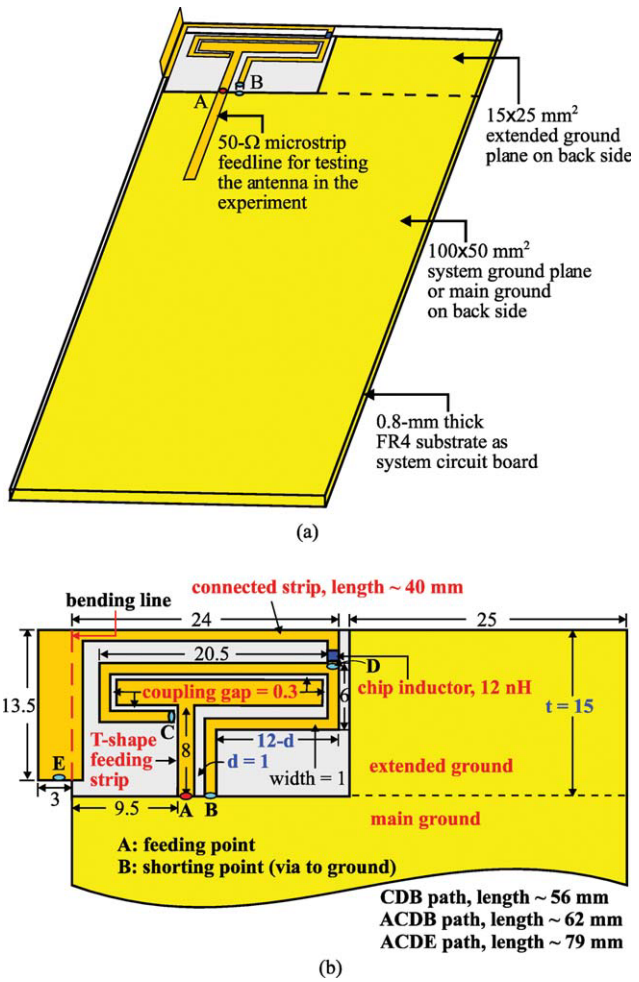

Figure 1 (a) Geometry of the proposed on-board small-size 7-band WWAN/LTE2300/2500 antenna for mobile phone application. (b) Dimensions of the proposed antenna. [Color figure can be viewed in the online issue, which is available at wileyonlinelibrary.com]

Also, easy tuning of the antenna's lower and upper bands to respectively cover the 824–960 and 1710–2690 MHz bands can be achieved for the proposed antenna, which is attractive for practical applications. Detailed operating principle of the proposed antenna is described in the article. Results of the fabricated prototype of the proposed antenna are presented and discussed. The radiation characteristics of the proposed antenna, including its radiation efficiency and SAR (specific absorption rate) [13, 19, 20] results with the presence of both the user's head and hand, are analyzed.

2. PROPOSED ANTENNA

Figure 1(a) shows the geometry of the proposed on-board small-size 7-band antenna for the WWAN/LTE2300/2500 operation in the mobile phone. Detailed dimensions of the proposed antenna are shown in Figure 1(b). Owing to the small size, the antenna is disposed on one corner only, without occupying the entire edge, of the system circuit board. In the study, a 0.8-mm thick FR4 substrate of relative permittivity 4.4 and loss tangent 0.024 is used as the system circuit board. On the back side of the FR4 substrate, a ground plane of length 100 mm and width 50 mm is printed to serve as the system ground plane or main ground plane of the mobile phone. An extended ground plane of length (t) 15 mm and width 25 mm connected to the main ground

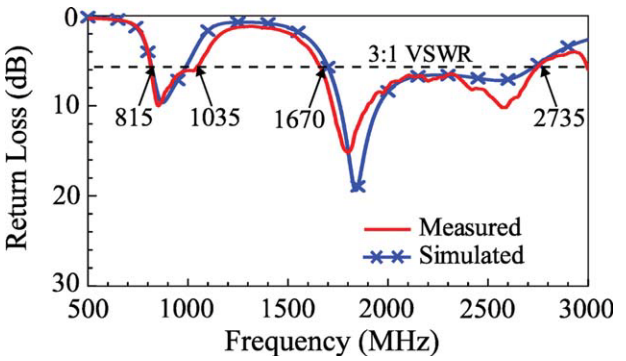

Figure 2 Measured and simulated return loss for the fabricated antenna. [Color figure can be viewed in the online issue, which is available at wileyonlinelibrary.com]

plane is also printed, which is placed close to the proposed antenna with a small isolation distance of 1 mm only. This extended ground plane can be used to accommodate associated components in the mobile phone, thereby increasing the effective size of the total ground plane in the mobile phone and also leading to efficient board space planning of the system circuit board. Detailed effects of the length t of the extended ground plane on the performances of the antenna are also studied with the aid of Figure 5 in the next section.

The antenna is mainly disposed on the no-ground portion of size 15×25 mm^2 by printing; except that the widened end section of the chip-inductor-loaded strip (section DE) is obtained by connecting a 0.2-mm thick metal plate of length 13.5 mm and width 3 mm to the printed end section of width 1 mm. This widened end section can lead to slight decrease in the resonant frequency of the excited resonant mode for the antenna's lower band. Notice that when a plastic housing (typical relative permittivity 3.0) [5, 11, 12, 21–23] is added to enclose the system circuit board to simulate as the mobile phone housing in practical applications, which can also cause some resonant frequency decrease in the excited resonant modes of the antenna, the end section in the proposed antenna is no longer required to be widened; that is, the added metal plate of length 13.5 mm and width 3 mm is not required. In this case, all the metal pattern of the proposed antenna can all be directly printed on the no-ground portion, making it easy to fabricate at low cost.

The antenna can be discomposed into two antenna elements: one is the coupled-fed loop antenna and the other is the coupled-fed shorted monopole antenna. The coupled-fed loop antenna comprises a T-shape feeding strip and a coupled loop strip (section CDB). The front terminal (point A) of the T-shape feeding strip is the antenna's feeding point. The coupled loop strip has a length of about 56 mm and is capacitively excited by the feeding strip through a coupling gap of 0.3 mm; this forms a coupled-fed loop antenna with a resonant loop path (ACDB path) of about 62 mm, which leads to the excitation of a 0.5-wavelength loop resonant mode at about 2.2 GHz. Further, this resonant mode can have a dual-resonant behavior [24–26] to achieve a very wide bandwidth of larger than 1 GHz to cover the desired operating band of 1710–2690 MHz. Also note that the performances of the coupled-fed loop antenna are strongly affected by the spacing d (1 mm in the proposed design) between the front section and end section of the loop antenna. Detailed effects of the spacing d are analyzed in Figure 4 in the next section.

For the coupled-fed shorted monopole antenna, it is formed by adding the chip-inductor-loaded strip to the coupled-fed loop antenna at point D. The chip inductor in the proposed design has a size of $0.5 \times 0.5 \times 1.0$ mm^3 and an inductance of 12 nH. The coupled-fed shorted monopole antenna consists of a radiating strip of section CDE, a T-shape coupling feed, and a shorted strip of section BD. Through the coupling gap of 0.3 mm, the monopole antenna also provides a resonant path of ACDE, which has a length of about 79 mm in this study. A 0.25-wavelength resonant mode can be generated by the coupled-fed shorted monopole antenna to form the antenna's lower band centered at about 925 MHz to cover the desired 824–960 MHz band. Also notice that, as discussed in Section 1, the loaded chip inductor of 12 nH effectively decreases the excited resonant mode to cover the desired operating band. The detailed effects of the loaded chip inductor are studied in the next section with the aid of Figure 3.

With the desired lower and upper bands respectively controlled by the coupled-fed loop antenna and the coupled-fed shorted monopole antenna, it is also found that the obtained two wide operating bands can be easily fine-adjusted respectively. This makes it easy for the proposed antenna to obtain the desired wide operating bands in practical mobile phone applications.

3. RESULTS AND DISCUSSION

The proposed antenna was fabricated and studied. Figure 2 shows the measured and simulated return loss for the fabricated antenna. The measured data are seen to agree with the simulated results obtained using Ansoft simulation software version 12 [27]. From the results, two wide operating bands are obtained. The lower band has a measured 3:1 VSWR (6-dB return loss) bandwidth of 220 MHz (815–1035 MHz), while the upper band has an even larger bandwidth of 1065 MHz (1670–2735 MHz).

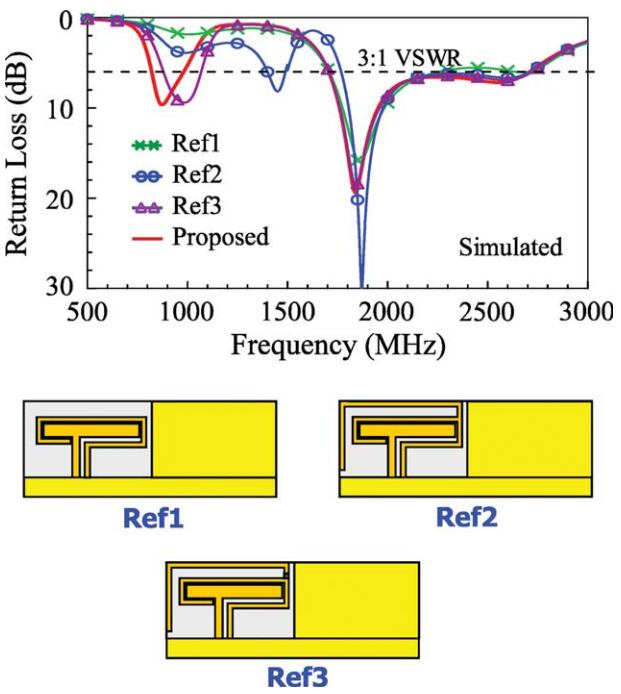

Figure 3 Simulated return loss for the proposed antenna, the case with the coupled-fed loop antenna only (Ref1), Ref1 with a simple strip connected (Ref2), and Ref1 with a chip-inductor-loaded strip connected (Ref3). Corresponding dimensions are the same as given in Figure 1. [Color figure can be viewed in the online issue, which is available at wileyonlinelibrary.com]

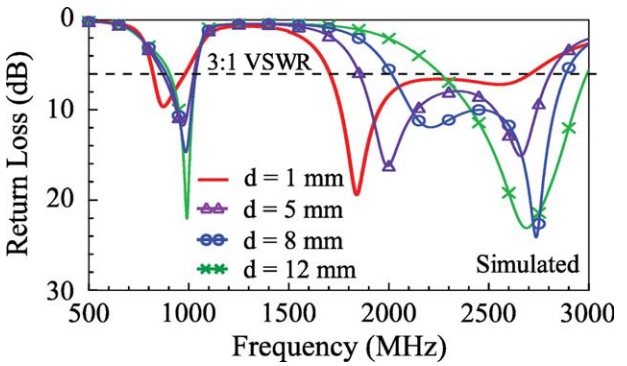

Figure 4 Simulated return loss as a function of the spacing d between the front section and end section of the coupled-fed loop antenna; other dimensions are the same as in Figure 1. [Color figure can be viewed in the online issue, which is available at wileyonlinelibrary.com]

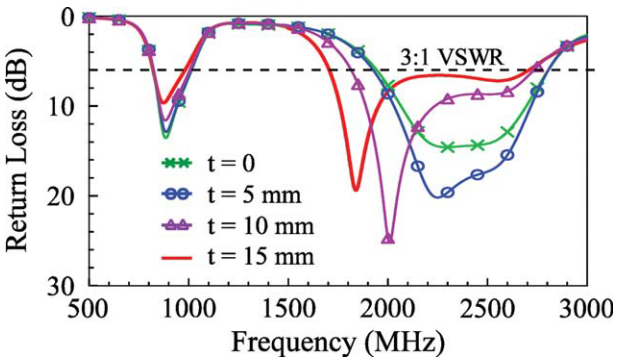

Figure 5 Simulated return loss as a function of the length t of the extended ground plane; other dimensions are the same as in Figure 1. [Color figure can be viewed in the online issue, which is available at wileyonlinelibrary.com]

The lower and upper bands respectively cover the GSM850/900 operation and the GSM1800/1900/UMTS/LTE2300/2500 operation; that is, the 7-band operation is obtained. Also notice that the 3:1 VSWR is widely used as the design specification of the internal mobile phone antenna for the WWAN and LTE operation.

The operating principle of the proposed antenna is analyzed in Figure 3. Results of the simulated return loss for the proposed antenna, the case with the coupled-fed loop antenna only (Ref1), Ref1 with a simple strip connected (Ref2), and Ref1 with a chip-inductor-loaded strip connected (Ref3) are shown in the figure. Notice that Ref1, Ref2, and Ref3 have the same corresponding dimensions as given in Figure 1 for the proposed antenna. For the four antennas studied in the figure, small variations in the antenna's upper band are seen. This behavior also confirms that the upper band is mainly controlled by the coupled-fed loop antenna (Ref1). However, the desired antenna's lower band cannot be excited by Ref1. When a simple strip is connected to Ref1 to form Ref2, a resonant mode at about 1500 MHz is generated. By further loading a chip inductor of 12 nH (Ref3), this resonant mode can be shifted to lower frequencies at about 1000 MHz. By widening the end section of the connected strip as seen in the proposed antenna, slight decreasing in the resonant frequency of this resonant mode to cover the desired operating band of 824–960 MHz can be achieved. It is also interesting to

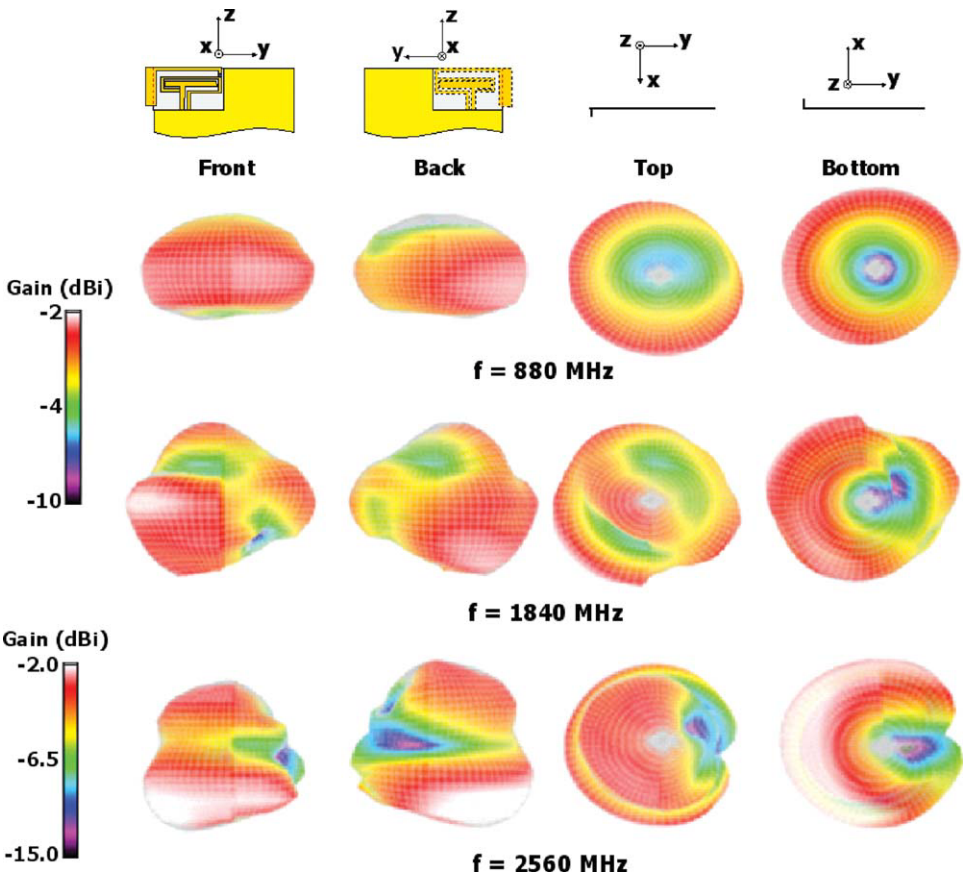

Figure 6 Measured three-dimensional (3-D) radiation patterns for the fabricated antenna. [Color figure can be viewed in the online issue, which is available at wileyonlinelibrary.com]

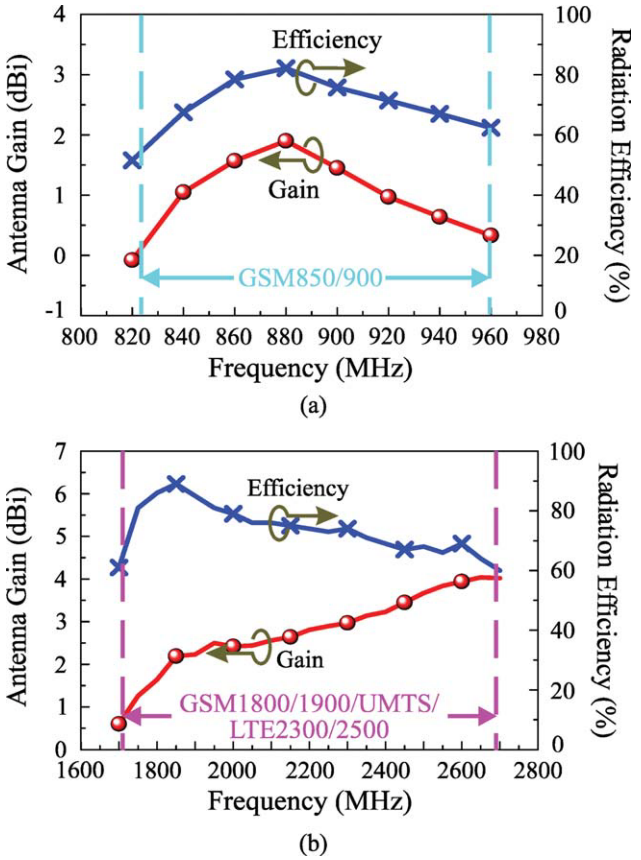

Figure 7 Measured radiation efficiency and antenna gain for the fabricated antenna. [Color figure can be viewed in the online issue, which is available at wileyonlinelibrary.com]

notice that the antenna's upper band is almost not affected by the connected chip-inductor-loaded strip to the coupled-fed loop antenna. This behavior is mainly because the loaded chip inductor contributes large inductance at frequencies in the upper band, which makes the chip inductor functions like an open circuit for frequencies in the upper band; thus, the connected strip will show small effects on the coupled-fed loop antenna operated in the antenna's upper band.

Effects of the spacing d between the front section and end section of the coupled-fed loop antenna are studied in Figure 4. Simulated results of the return loss for the spacing d varied from 1 to 12 mm are shown in the figure. For $d = 12$ mm, it indicates that the end section of the loop antenna is straight in shape, whereas $d = 1$ mm is the case shown in Figure 1 for the proposed antenna. It can be seen that there are large effects on both the antenna's lower and upper bands. By selecting a smaller spacing, which increases the coupling between the front section and end section of the loop antenna, the upper band can be shifted to lower frequencies to cover the desired 1710–2690 MHz band. At lower frequencies, since the antenna is operated as a coupled-fed shorted monopole antenna and the spacing d also affects the coupling between the feeding strip and the shorting strip, some effects on the lower band are also seen.

Effects of the length t of the extended ground plane are studied in Figure 5. Simulated results of the return loss for the length t varied from 0 to 15 mm are shown. Again, some effects on both the lower and upper bands are seen. When the extended ground plane is not present ($t = 0$), the lower-band bandwidth can be improved; while for $t = 15$ mm (the proposed antenna), the obtained lower-band bandwidth is the smallest. However, the obtained bandwidth for $t = 15$ mm is wide enough for the GSM850/900 operation. However, the obtained upper-band bandwidth is increased with increasing length of the extended ground plane. This is largely because the proposed antenna can be in compact integration with the extended ground plane, and furthermore, the coupling between the antenna and the extended ground plane has been taken into consideration in the design of the proposed antenna.

Figure 6 shows the measured three-dimensional (3-D) radiation patterns for the fabricated antenna. Typical radiation patterns, at 880, 1840, and 2560 MHz, are shown. At each frequency, four radiation patterns seen from four different directions of front, back, top, and bottom are presented. At 850 MHz, the obtained radiation patterns are similar to those of a traditional half-wavelength dipole antenna. For higher frequencies at 1840 and 2560 MHz, the obtained radiation patterns become more directive and also asymmetric with respect to the z axis. This behavior is related to the proposed antenna disposed on only one corner of the system circuit board and the presence of the extended ground plane in the close proximity of the antenna. Effects of this asymmetric structure on the antenna's radiation characteristics become significant at higher frequencies, which contribute to the asymmetric radiation patterns seen at higher frequencies. The measured results of the radiation efficiency and antenna gain are presented in Figure 7. The measured radiation efficiency is respectively about 53–81% and 60–90% for frequencies over the lower band [Fig. 7(a)] and the upper band [Fig. 7(b)].

The measured antenna gain is about 0.1–1.8 dBi and 0.6–4.0 dBi over the lower and upper bands, respectively. Notice that over the upper band as seen in Figure 7(b), the antenna gain increases with increasing frequencies. This is related to the asymmetric radiation patterns seen in Figure 6 at higher frequencies.

TABLE 1 Simulated Results of the Return Loss, Radiation Efficiency and, SAR for the Proposed Antenna in Free Space, with the Head Only, and with the Head and Hand

	Free space		Head only			Head and hand		
Frequency (MHz)	RL (dB)	Effi. (%)	RL (dB)	Effi. (%)	SAR (W/kg)	RL (dB)	Effi. (%)	SAR (W/kg)
859	8.9	79	8.4	22	1.53	9.3	5	1.68
925	8.2	76	6.6	21	1.45	6.5	4	1.56
1795	16.9	88	12.2	40	1.10	13.8	11	1.23
1925	9.3	81	7.9	38	0.93	9.4	12	1.30
2045	6.6	73	5.7	35	0.76	6.5	12	1.14
2350	6.7	73	5.3	37	0.69	4.9	14	0.85
2595	7.0	69	6.2	39	0.70	6.7	17	1.24

Results are obtained using SEMCAD [28] and based on the simulation models given in Figure 8.

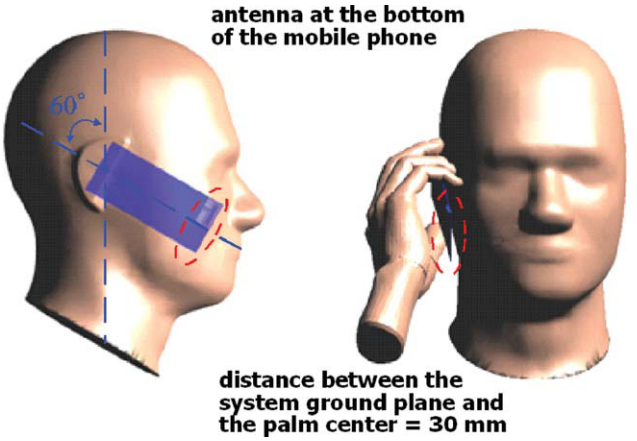

Figure 8 SAR simulation models provided by SEMCAD for two cases of the head only and the head and hand. [Color figure can be viewed in the online issue, which is available at wileyonlinelibrary.com]

Finally, the SAR results of the proposed antenna are studied using the SAR simulation models provided by SEMCAD version 14 [28]. Both the user's head and hand presence are considered, and the 1-g SAR values for the head only and the head and hand are given in Table 1. The simulated results of the return loss obtained by SEMCAD for the proposed antenna in free space, with the head only, and with the head and hand are shown in Figure 9 for comparison. The corresponding results of the return loss and radiation efficiency (mismatch considered) at the testing frequencies for the SAR values are also listed in Table 1. Also note that in the SAR testing, the antenna is mounted at the bottom of the mobile phone as shown in Figure 8 for decreased SAR results [10–14], and the grip of the hand phantom on the mobile phone is shown in the figure, with the distance between the system ground plane and the palm center set to 30 mm, which is reasonable distance as studied in [13]. The input power for the SAR testing is 24 dBm at 859 and 925 MHz for the GSM850/900 operation and 21 dBm at 1795, 1925, 2045, 2350, and 2595 MHz for the GSM1800/1900/UMTS/LTE2300/2500 operation.

From the results shown in Figure 9, small variations in the obtained return loss are seen for the presence of the head and hand phantoms. However, as seen in Table 1, large effects on the radiation efficiency are observed. For the head only, the radiation efficiency is decreased by about 5.5 dB at lower frequencies (859 and 925 MHz) and about 2.5–3.5 dB at higher frequencies (1795–2595 MHz). For both the head and hand presence, much larger decrease in the radiation efficiency is seen; the radiation efficiency is decreased by about 12.0–12.8 dB at lower frequencies and about 6.0–9.0 dB at higher frequencies, compared with those in free space. The large decrease in the radiation efficiency is because the user's head and hand are both lossy materials, which can absorb large radiated power of the antenna in the mobile phone.

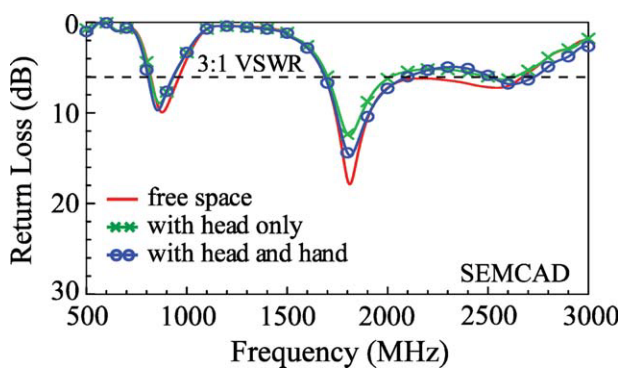

Figure 9 Simulated return loss (SEMCAD) for the proposed antenna in free space, with the head only, and with the head and hand. [Color figure can be viewed in the online issue, which is available at wileyonlinelibrary.com]

For the 1-g SAR values, they are slightly higher for the head and hand than for the head only. The SAR value at 859 MHz for the head and hand is also slightly higher than the SAR limit of 1.6 W/kg. This needs to be considered for practical applications of the proposed antenna, when the user's hand is required to be included in the SAR testing in the near future. However, notice that the mobile phone housing which is made from the lossy plastic materials is not included in the SAR testing here. Smaller SAR values than those obtained in the paper can hence be expected. However, at higher frequencies, although some increases in the SAR values for the head and hand are also obtained than those for the head only, all the obtained SAR values for both the head only and the head and hand are well below the SAR limit of 1.6 W/kg. The obtained SAR results suggest that the proposed antenna is promising for practical mobile phone applications, even for the case of the user's hand included in the SAR testing.

4. CONCLUSION

An on-board 7-band WWAN/LTE mobile phone antenna with small occupied board size and compact integration with the nearby ground plane has been proposed. The antenna has been fabricated and studied. Although occupying a small board space of 15×25 mm^2 (375 mm^2) on the system circuit board of the mobile phone and closely spaced to the nearby ground plane extended from the system ground plane, the antenna provides two wide operating bands to respectively cover the GSM850/900 and the GSM1800/ 1900/UMTS/LTE2300/2500 operations. In addition, acceptable radiation characteristics for frequencies over the seven operating bands have been obtained. The SAR results for the 1-g head only and the 1-g head and hand have also been studied. The results suggest that the proposed antenna is promising to meet the required 1-g SAR limit of 1.6 W/kg for practical mobile phone applications.

REFERENCES

1. R.A. Bhatti, Y.T. Im, J.H. Choi, T.D. Manh, and S.O. Park, Ultra-thin planar inverted-F antenna for multistandard handsets, Microwave Opt Technol Lett 50 (2008), 2894–2897.
2. K.L. Wong and T.W. Kang, GSM850/900/1800/1900/UMTS printed monopole antenna for mobile phone application, Microwave Opt Technol Lett 50 (2008), 3192–3198.
3. C.L. Tang and S.C. Lai, Multi-function IC antenna Design and Fabrication, Proceedings of Asia-Pacific Microwave Conference, Singapore, 2009, Session TU4A, Paper no. 1741.
4. H. Rhyu, J. Byun, F.J. Harakiewicz, M.J. Park, K. Jung, D. Kim, N. Kim, T. Kim, and B. Lee, Multi-band hybrid antenna for ultra-thin mobile phone applications, Electron Lett 45 (2009), 773–334.
5. Y.W. Chi and K.L. Wong, Very-small-size folded loop antenna with a band-stop matching circuit for WWAN operation in the mobile phone, Microwave Opt Technol Lett 51 (2009), 808–814.
6. T.W. Kang and K.L. Wong, Chip-inductor-embedded small-size printed strip monopole for WWAN operation in the mobile phone, Microwave Opt Technol Lett 51 (2009), 966–971.
7. C.T. Lee and K.L. Wong, Uniplanar coupled-fed printed PIFA for WWAN/WLAN operation in the mobile phone, Microwave Opt Technol Lett 51 (2009), 1250–1257.

8. K.L. Wong and W.Y. Chen, Small-size printed loop antenna for penta-band thin-profile mobile phone application, Microwave Opt Technol Lett 51 (2009), 1512–1517.
9. C.H. Chang and K.L. Wong, Small-size printed monopole with a printed distributed inductor for penta-band WWAN mobile phone application, Microwave Opt Technol Lett 51 (2009), 2903–2908.
10. C.H. Chang and K.L. Wong, Printed λ/8-PIFA for penta-band WWAN operation in the mobile phone, IEEE Trans Antennas Propag 57 (2009), 1373–1381.
11. Y.W. Chi and K.L. Wong, Quarter-wavelength printed loop antenna with an internal printed matching circuit for GSM/DCS/PCS/UMTS operation in the mobile phone, IEEE Trans Antennas Propag 57 (2009), 2541–2547.
12. W.Y. Chen and K.L. Wong, Small-size coupled-fed shorted T-monopole for internal WWAN antenna in the slim mobile phone, Microwave Opt Technol Lett 52 (2010), 257–262.
13. C.H. Li, E. Ofli, N. Chavannes, and N. Kuster, Effects of hand phantom on mobile phone antenna performance, IEEE Trans Antennas Propag 57 (2009), 2763–2770.
14. M.R. Hsu and K.L. Wong, Seven-band folded-loop chip antenna for WWAN/WLAN/WiMAX operation in the mobile phone, Microwave Opt Technol Lett 51 (2009), 543–549.
15. S. Sesia, I. Toufik, and M. Baker (Eds.), LTE, The UMTS Long Term Evolution: From Theory to Practice, Wiley, New York, 2009.
16. C.T. Lee and K.L. Wong, Planar monopole with a coupling feed and an inductive shorting strip for LTE/GSM/UMTS operation in the mobile phone, IEEE Trans Antennas Propag, in press.
17. J. Thaysen and K. B. Jakobsen, A size reduction technique for mobile phone PIFA antennas using lumped inductors, Microwave J 48 (2005), 114–126.
18. J. Carr, Antenna Toolkit, second edition, Newnes, Oxford, U.K., 2001 pp. 111–112.
19. American National Standards Institute (ANSI), Safety levels with respect to human exposure to radio-frequency electromagnetic field, 3 kHz to 300 GHz, ANSI/IEEE standard C95.1, April 1999.
20. J.C. Lin, Specific absorption rates induced in head tissues by microwave radiation from cell phones, Microwave 40 (2001), 22–25.
21. W.Y. Li and K.L. Wong, Small-size WWAN loop chip antenna for clamshell mobile phone with hearing-aid compatibility, Microwave Opt Technol Lett 51 (2009), 2327–2335.
22. K.L. Wong and C.H. Huang, Printed loop antenna with a perpendicular feed for penta-band mobile phone application, IEEE Trans Antennas Propag 56 (2008), 2138–2141.
23. C.H. Wu and K.L. Wong, Hexa-band internal printed slot antenna for mobile phone application, Microwave Opt Technol Lett 50 (2008), 35–38.
24. K.L. Wong and C.H. Huang, Bandwidth-enhanced internal PIFA with a coupling feed for quad-band operation in the mobile phone, Microwave Opt Technol Lett 50 (2008), 683–687.
25. K.L. Wong and C.H. Huang, Printed PIFA with a coplanar coupling feed for penta-band operation in the mobile phone, Microwave Opt Technol Lett 50 (2008), 3181–3186.
26. C.H. Chang and K.L. Wong, Internal coupled-fed shorted monopole antenna for GSM850/900/ 1800/1900/UMTS operation in the laptop computer, IEEE Trans Antennas Propag 56 (2008), 3600–3604.
27. http://www.ansoft.com/products/hf/hfss/. This is the official web site of the Ansoft Corporation HFSS.
28. http://www.semcad.com. This is the official web site of the SEMCAD, Schmid & Partner Engineering AG (SPEAG).

ERRATUM: SINGLE-SHOT ALL-OPTICAL SAMPLING OSCILLOSCOPE USING A POLARIZATION-MAINTAINING RESONATOR FOR PULSE REPLICATION

Matěj Komanec,[1] Pavel Honzátko,[2] and Stanislav Zvánovec[1]
[1] Faculty of Electrical Engineering, Department of Electromagnetic Field, Czech Technical University in Prague, Technicka 2, 166 27 Prague 6, Czech Republic; Corresponding author: komanmat@fel.cvut.cz
[2] Institute of Photonics and Electronics, Chaberská 57, 182 51 Prague, Czech Republic

Received 5 February 2010

ABSTRACT: *Originally published Microwave Opt Technol Lett 52: 2452–2456, 2010.* © 2010 Wiley Periodicals, Inc. Microwave Opt Technol Lett 52: 2853, 2010; Published online in Wiley Online Library (wileyonlinelibrary.com). DOI 10.1002/mop.25620
(Original article DOI 10.1002/mop.25509)

It has been brought to our attention that the authors' names appeared incorrectly in the original publication of this article: their first names and surnames were incorrectly transposed. The authors' names are correct as listed above.

We apologize for any inconvenience this error may have caused.